Pressure distribution around a near-wall circular cylinder subjected to steady current

M. A. Salehi[1], S. Mazaheri[2], M. H. Kazeminezhad[3]

[1] Ocean Engineering and Technology Research Center, Iranian National Institute for Oceanography and Atmospheric Sciences, Tehran, Iran, mascivil9@gmail.com

[2] Ocean Engineering and Technology Research Center, Iranian National Institute for Oceanography and Atmospheric Sciences, Tehran, Iran, said.mazaheri@inio.ac.ir

[3] Ocean Engineering and Technology Research Center, Iranian National Institute for Oceanography and Atmospheric Sciences, Tehran, Iran, mkazeminezhad@inio.ac.ir

ARTICLE INFO

ABSTRACT

Flow around a circular cylinder near plane wall has been simulated using Open source CFD codes of OpenFOAM in different flow regimes (Re=100, 200, 3900) and different gap ratios (G/D= ∞, 1, 0.5, 0.2). Time-averaged pressure coefficients around a circular cylinder computed and compared with each others in different cases. Other features of flow including drag and lift coefficients, Strouhal number, separation angle and stagnation angle are also computed to describe the state of flow better. It has been shown that pressure distribution around the circular cylinder can be utilized to describe the variations in hydrodynamic force coefficients as well as other features of wake flow such as separation and vortex shedding phenomenon near a plane boundary. Plane wall effects on pressure distribution in different flow regimes investigated and it was found that the inception of vortex shedding suppression can be deduced from pressure distribution pattern, through pressure gradient between free-stream-side and wall-side of cylinder. In addition, a rapid increase in the maximum value of positive pressure coefficient can be concluded.

1. Introduction

Flow around circular cylinders near plane boundary has been a subject of interest for researchers because of its vast practical applications in ocean and offshore engineering such as offshore pipelines in various conditions particularly in free spans and near sea beds. Interaction between pipeline and fluid near a sedimentary seabed can promote erosion and free spans, which makes the pipeline vulnerable to vortex induced vibrations. Vortex shedding phenomenon leads to vortex induced vibration of a cylinder subjected to cross flow, which is undesirable due to fatigue concerns.

Measurements of the pressures and forces around a circular cylinder and their fluctuations can be used to describe the features of the interference between cylinder and plane and help control the occurrence of vortex shedding.

Zdravkovic, [1], categorized states of flow around a circular cylinder and its wake based on flow regimes and Reynolds number, according to Table 1.

Transition in Wake, Transition in Shear Layers and Transition in Boundary Layers, are shown in figure 2:

Table 1. States of flow around a circular cylinder in different flow regimes, [1]

| State			Regime	Re changes
L	Laminar	1	No-Separation	0 to 4-5
		2	Closed Wake	4-5 to 30-48
		3	Periodic Wake	30-48 to 180-200
TrW	Transition in Wake	1	Far-Wake	180-200 to 220-250
		2	Near-Wake	220-250 to 350-400
TrSL	Transition in Shear Layers	1	Lower	350-48 to 1k-2k
		2	Intermediate	1k-2k to 20k-40k
		3	Upper	20k-40k to 100k-200k
TrBL	Transition in Boundary Layers	0	Pre-critical	100k-200k to 300k-340k
		1	Single Bubble	300k-340k to 380k-400k
		2	Two Bubble	380k-400k to 500k-1M
		3	Supercritical	500k-1M to 3.5M-6M
		4	Post-critical	3.5M-6M to ?
T	Fully Turbulent	1	Invariable	? to ∞
		2	Ultimate	
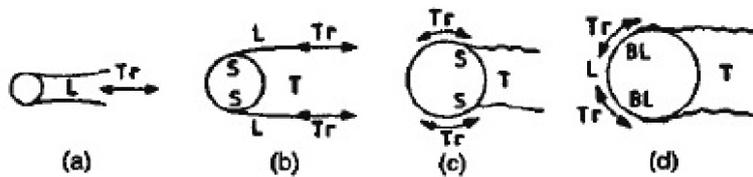
Figure 2- (a) Transition in Wake, (b) Transition in Shear Layers, (c),(d) Transition in Boundary Layers, [1]

First measurements of pressure distribution in laminar state of flow were carried out by Thom [2] in water and Homann [3] in oil. The single curve is drawn for the range $36 < Re < 107$ shows that there is negligible effect of Re on the base pressure, C_{pb}. Thom, [2], and Homann, [3], measured mean pressure distribution around a circular cylinder in the TrW state of flow. There is a branching of curves beyond $\theta_s = 70°$ and related variation in C_{pb}, where θ_s is the separation angle The separation angle θ_s can be estimated from the inflection in the curves to be in the range $95° < \theta_s < 115°$. Note that higher values of θ_s correspond to lower Re and vice versa. Williamson and Roshko, [4], measured only the base pressure in the range $50 < Re < 350$ that covers the L3, TrWl and part of the TrW2 flow regimes. The laminar periodic regime, L3, shows a continuous increase in $-C_{pb}$ related to a decrease in L_f, the shortest length of eddy formation The first discontinuity at Re = 170 coincides with the appearance of fingers and the related drawing back of dye into the near-wake. Further shortening of Lf in TrWl leads to the increase in $-C_{pb}$ which leads at Re = 270, to $(-C_{pb})$max, and (L_f)min.

Bearman and Zdravkovic, [5], investigated flow around a circular cylinder at various heights above a plane boundary experimentally and found out flow around a circular cylinder near plane boundary depends on cylinder Reynolds number, gap ratio (G/D) and characteristics of the boundary layer. Distributions of mean pressure around the cylinder and along the plate were measured at a Reynolds number, based on cylinder diameter, of 4.5×10^5. Spectral analysis of hot-wire signals demonstrated that regular vortex shedding was suppressed for all gaps less than about 0.3 cylinder diameters and for gaps greater than 0.3 the Strouhal number was found to be remarkably constant. Zdravkovic, [6], measured the lift and drag forces on circular cylinders fitted with end plates in a wind tunnel. The gap between the cylinder and the wall, G, the thickness of the turbulent boundary layer along the wall, δ, and Re are varied in the following ranges: $0 < G/D < 2$, $12 < \delta/D < 0.97$ and $4.8 \times 10^4 < Re < 3 \times 10^5$. The lift and drag coefficients are presented in terms of a new variable G/δ. It was found that the lift coefficient is governed by the gap to diameter ratio *G/D* while the drag coefficient is dominated by the ratio of gap to thickness of the boundary layer, *G/δ*.

Pressure distribution around a cylinder near a plane boundary relates to displacement of stagnation point in front of cylinder toward gap and displacement of separation points around the cylinder. Since the flow structure around the separation point is the source of vortical instability in the wake, vortex shedding depends on the flow separation from the cylinder boundary layer.

Wu et al. ,[7], investigated The separation point of the flow around a circular cylinder numerically and experimentally in the regime of Reynolds number less than 280. It reveals that the variations of the time-averaged separation angles with Reynolds number can be represented by a simple linear θ_s–$Re^{-1/2}$ relationship for $10 < Re < 200$.

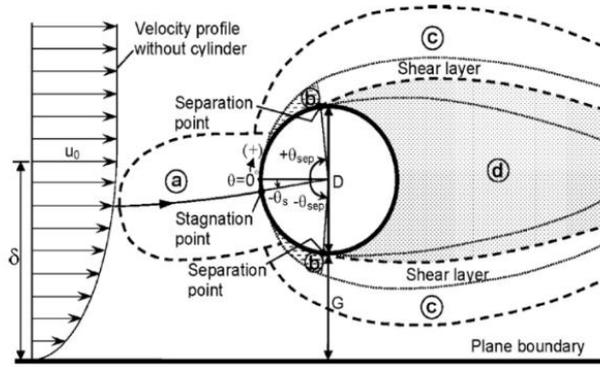Some of near wall flow field parameters around circular cylinder have been illustrated in figure 1.

Figure 1. Definition of near wall flow field parameters around circular cylinder, [8]

According to above review, comparing pressure distribution around a circular cylinder near a plane boundary, in addition to provide information for hydrodynamic force computations, presents insight on near-wake characteristics of flow near plane boundary. In this study, pressure coefficient is defined as:

$$C_p = \frac{P - P_s}{\frac{1}{2}\rho U_\infty^2}$$

Where P is the pressure measured on the surface of the cylinder, P_s is the hydrostatic pressure taken from the cylinder position, ρ is the density of the water and U_∞ is the far field flow velocity.

In this study, three dimensional flow around a circular cylinder near plane wall has been simulated using Open source CFD codes of OpenFOAM in different flow regimes (Re=100, 200, 3900) and different gap ratios (G/D= ∞, 1, 0.5, 0.2).

Time-averaged pressure distribution around a circular cylinder presented graphically according to Gap ratio, G/D, and compared for Re=100,200 and 3900. The results show that the pressure distribution pattern can be used to describe near-wake flow around a circular cylinder, and the variation of flow configurations subjected to different geometrical and hydrodynamic situations.

Governing Equations:

Time averaged Navier-Stokes equations including continuity equation are the governing equations for incompressible fluid flow:

$$\frac{\partial u_i}{\partial x_i} = 0 \qquad (2)$$

$$\rho\left(\frac{\partial u_i}{\partial t} + u_j\frac{\partial u_i}{\partial x_i}\right) = B_i - \frac{\partial p}{\partial x_i} + \mu\frac{\partial^2 u_i}{\partial x_j \partial x_j} + \frac{\partial}{\partial xj}\left(-\rho u_i' u_j'\right) \qquad (3)$$

$$\tau = \left(-\rho u_i' u_j'\right) \qquad (4)$$

Where u, p, ρ, υ, B and τ are the velocity, pressure, density, kinematics viscosity, body forces and Reynolds stress, respectively. K-ω SST, a two-

equation eddy-viscosity turbulence model has been employed to close the system of equations. K-ω SST, presented by Menter (1994), is a variant of the standard k–ω model. Combines the original Wilcox k-w model for use near walls and the standard k–ε model away from walls using a blending function, and the eddy viscosity formulation is modified to account for the transport effects of the principle turbulent shear stress This turbulence model solves one transport equation for the turbulent kinetic energy, k, and one transport equation for the dissipation per unit kinetic energy, ω, also regarded as a turbulent frequency scale. (1)

Computational Domain:

Computational domain of 30D×20D×10D dimensions with totally hexahedral meshes was created. Cylinder diameter "D" is set equal to 10cm. Boundary conditions for far field and near the plane wall cases are shown in Fig.2.
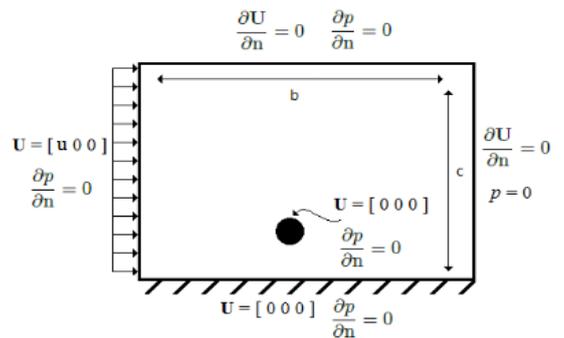

Figure 2. Boundary conditions for flow around circular cylinder near the wall

Numerical Model

IcoFoam, the basic laminar incompressible solver of OpenFOAM has been used for Re=100,200 while for Re=3900, PimpleFOAM (merged PISO-SIMPLE algorithm), which is a large time-step transient model has solver for incompressible flow alongside K-ω SST turbulence been employed to solve the equations.

Model Verification:

Comparison of simulation results for flow around circular cylinder far from plane boundary, including drag coefficient, positive maximum figure of lift coefficient and Strouhal number were considered and compared with those obtained by Cao and Wan, [9],

Williamson, [10], Norberg, [11], and Rosetti et al, [12], showed good agreement, Table 1. Also the computational velocity fields from the present simulations are compared with the experimental results obtained from PIV measurements of Oner et al., [13], for further validation of the numerical code.

Table 2. Comparison of C_d, $C_l(max)$ and S_t parameters for Re=100,200

	Re=100			Re=200		
	C_d	C_l	S_t	C_d	C_l	S_t
Present study	1.26	0.11	0.16	1.2	0.31	0.19
Cao and Wan	1.39	-	0.16	1.4	-	0.19
Williamson	-	-	0.16	-	-	0.19
Norberg	-	0.12	0.16	-	0.32	0.18
Rosetti et al.	1.41	-	0.17	1.3	-	0.2

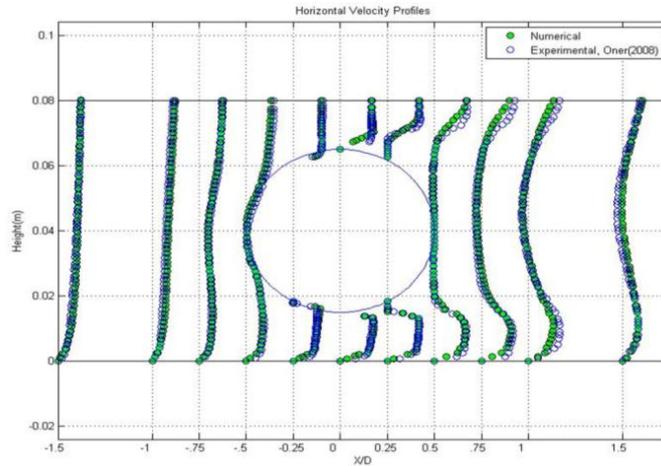**Figure 3.comparison of horizontal velocity profiles of present numerical simulation and experimental study of Oner et. al, [13] for G/D=0.3 and Re=9500**

Results and Discussion

Tables 2,3 and 4 present the results of 3-D computations including hydrodynamic drag, cd(mean) and lift coefficients, cl(rms), Strouhal number (st), gap to boundary layer thickness ratio (G/δ), Separation angle, Stagnation angle and base pressure, Cpb, for

different gap ratios and Re=100, 200 and 3900. It has been observed that for the range of G/δ < 0.45 there is a high possibility of vortex shedding suppression. The thickness of the boundary layer, δ, can be determined by measuring the velocity profile of the boundary layer at the cylinder location.

Table 2: 3-D numerical results of flow around circular cylinder far from and near the wall for Re=100

Re=100	G/D= ∞	G/D=1	G/D=0.5	G/D=0.2
cd(mean)	1.269	1.61	1.405	1.165
cl(rms)	0.111	0.2	0.163	0.598
st	0.161	0.183	0.092*	0.196*
G/δ	-	1.042	0.521	0.208
separation angle	114.72	98.97	95.51	92.29
stagnation angle	0	-2.2	-5.5	-9
Cpb	-0.53	-0.64	-0.52	-0.56

Table 3: 3-D numerical results of flow around circular cylinder far from and near the wall for Re=200

Re=200	G/D= ∞	G/D=1	G/D=0.5	G/D=0.2
cd(mean)	1.208	1.518	1.425	1.143
cl(rms)	0.306	0.492	0.342	0.417
st	0.192	0.209	0.1	0.25*
G/δ	-	1.19	0.595	0.238
separation angle	108.07	98.97	95.51	92.29
stagnation angle	0	-2.2	-8.1	-11
Cpb	-0.69	-0.86	-0.72	-0.57

Table 4: 3-D numerical results of flow around circular cylinder far from and near the wall for Re=3900

Re=3900	G/D= ∞	G/D=1	G/D=0.5	G/D=0.2
cd(mean)	1.281	1.712	1.544	1.238
cl(rms)	0.677	1.032	0.896	0.51
st	0.214	0.18	0.092	0.04*
G/δ	-	2.174	1.087	0.435
separation angle	98.98	98.97	92.75	85.5
stagnation angle	0	-2.2	-14.7	-6.8
Cpb	-1.15	-1.71	-1.13	-0.91

Time-averaged pressure distribution around a circular cylinder and separation points for all cases, cylinder far from and near the wall, have been presented in figures 4, 5 ,7 and 8. Pressure distribution has been represented by pressure coefficient, C_p. Pressure distribution pattern around a circular cylinder with gap ratio of G/D=1 in current study is similar to Bearman and Zdravkovic study, [5] , for G/D=1 and different Reynolds number, Figures 5 and 6.
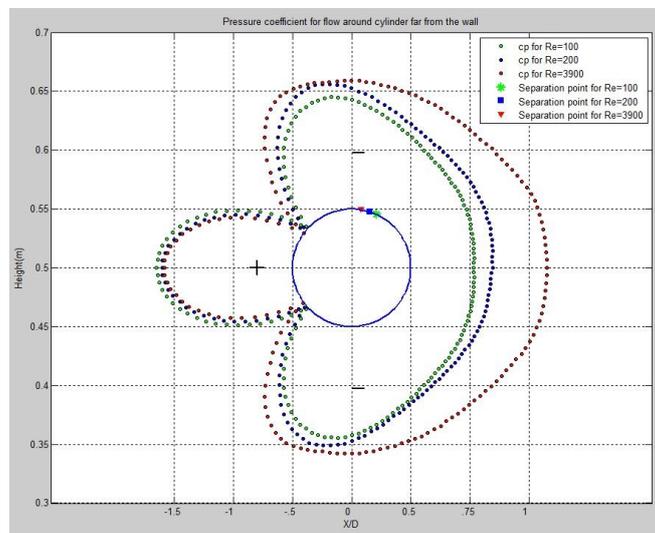

Figure 4. Pressure coefficient distribution around circular cylinder at G/D=∞, for Re=100,200,3900
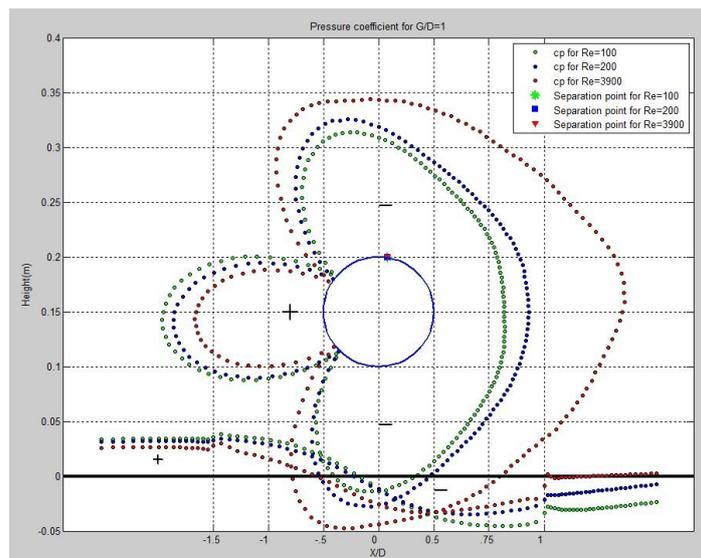

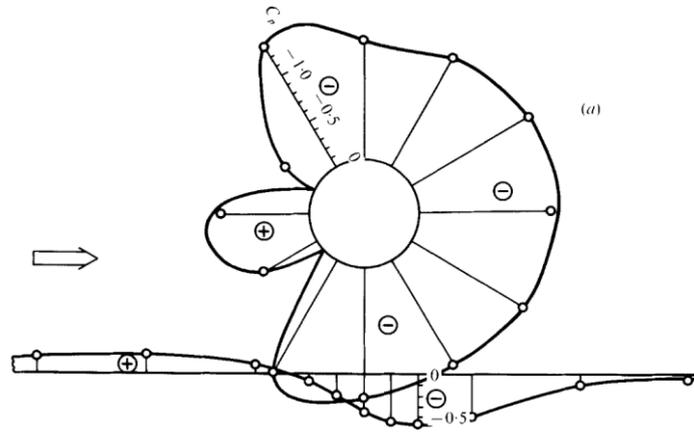**Figure 5. Pressure coefficient distribution around circular cylinder at G/D=1, for Re=100,200,3900**

Figure 6. Pressure coefficient distribution around circular cylinder at G/D=0.1, for Re=4.5×10⁴, [5]
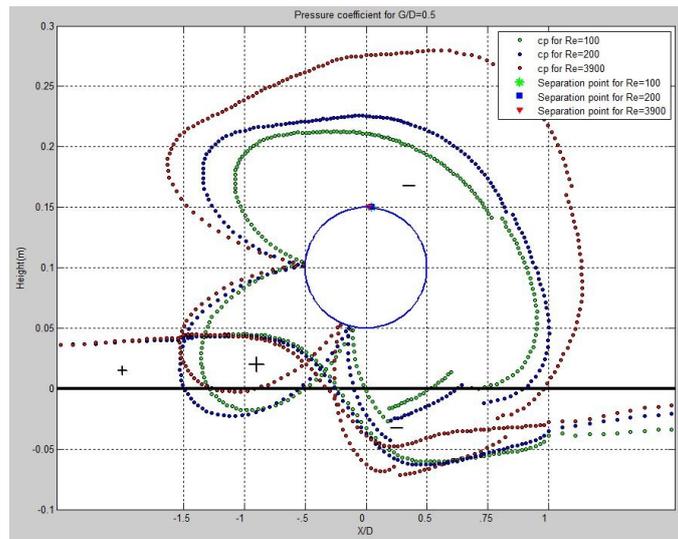

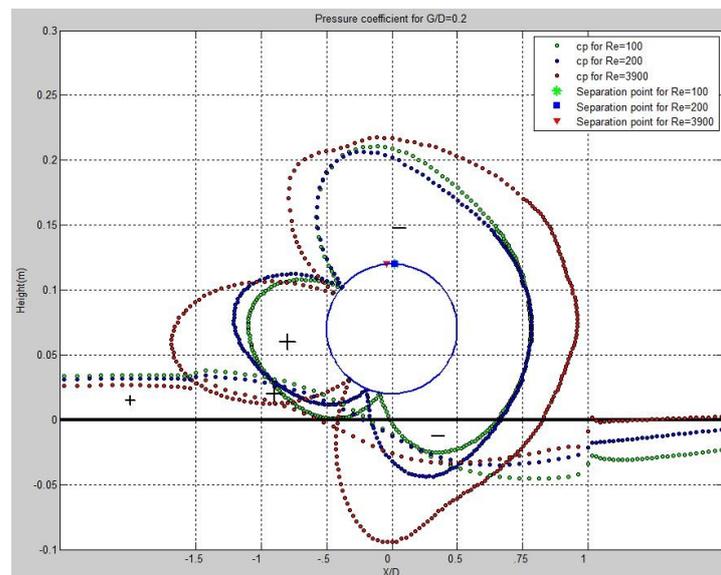**Figure 7. Pressure coefficient distribution around circular cylinder at G/D=0.5, for Re=100,200,3900**

Figure 8. Pressure coefficient distribution around circular cylinder at G/D=0.2, for Re=100,200,3900

It is seen that bell-shaped pressure coefficient distribution pattern includes a smaller section of positive pressure coefficient in front of cylinder and a bigger section of negative pressure coefficient around the other parts of the cylinder perimeter. In all cases,

far from and near the wall, the symmetry of pressure coefficient around the stagnation point has been observed. Investigation of pressure coefficient around the cylinder shows that by reducing gap ratio, G/D, higher lift force pushes the cylinder upward. The

amount of lift increase is less pronounced when vortex shedding suppressed or boundary layer is thicker. By increasing G/D, positive and negative values of pressure coefficients around the cylinder decreased, hence mean lift force on the cylinder decreases too. In high inference between the cylinder and the wall, i.e. smaller G/D, and when boundary layers around the cylinder and the wall overlap more fittingly, the maximum of positive pressure coefficient increases and moves downstream.

Vortex shedding suppression can be predicted by monitoring the variations of pressure distribution around the circular cylinder near the boundary, hence suppression can be preceded by modifying the pressure distribution patterns. Vortex shedding suppression observed in 4 cases, all of three cases of flow around a circular cylinder near wall with G/D=0.2 and the other one for flow around a circular cylinder near wall with G/D=0.5 and Re=100. For these cases, a sustained negative pressure is observed at the free-stream side of the cylinder and a less pronounced negative pressure is observed at the wall-side of the cylinder. The maximum of positive pressure coefficient experiences a chamber in shape and a bit of decrease in value while suppression occurs. Insufficient gradient of pressure between free-stream side and wall-side of cylinder leads to a static and stable state of shear layers, which prevents the process of vortex shedding to proceed or in intense condition, i.e. very low G/δ, shear layers don't even manage to roll-up. Time-averaged streamlines around a circular cylinder for G/D=0.2 and Re=100 demonstrates the latter description, figure 9.
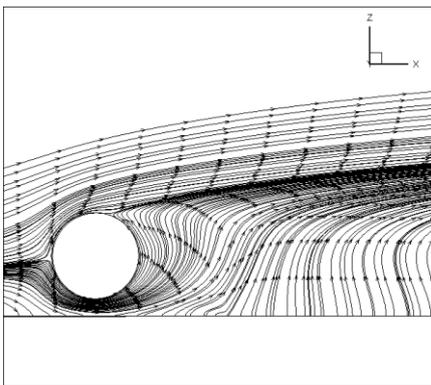

Figure 9. Time-averaged streamlines for flow around a circular cylinder for G/D=0.2 and Re=100

Based on figures 4, 5 ,7 and 8, it can be observed that upper separation point moves counter-clockwise by increasing Reynolds number (decrease in separation angle, θ_s), in a fixed gap ratio. Also in a fixed Reynolds number, upper separation point moves upward by decreasing G/D (decrease in separation angle, θ_s). Upward displacement of upper separation point by approaching the wall ,can be described by the growing stream-wise pressure gradient induced by the gap flow. Separation occurs when skin friction

vanishes, where velocity gradient at the wall becomes zero. The effect of the boundary layer on the pressure distribution can be attributed to the existence of the velocity gradient in the boundary layer. Drag coefficient consists of friction drag and form (pressure) drag and major fluctuations of drag force around circular cylinder relates to form drag in a distinct flow regime. When drag coefficient, a function of pressure distribution, rapidly decreases, it can be deduced that friction drag increases with respect to form drag and velocity gradient reaches its maximum value, hence separation of boundary layer does not proceed, i.e. vortex shedding suppression occurs.

Stagnation point is the correspondent point on the cylinder surface to the maximum of positive pressure coefficient. It is shown that stagnation point moves toward wall by increasing Reynolds number (decrease in stagnation angle).

According to tables 2, 3 and 4, Mean drag coefficient, Cd(mean) generally increases with increasing Gap ratio, G/D. But from G/D=1 to G/D=∞, considering the ratio of gap distance to cylinder boundary layer thickness, G/δ, reduce in drag coefficient observed, which is the result of the cylinder exit from the influence zone of plane wall`s boundary layer. Oscillating lift coefficient, represented by Cl(rms), root mean square of lift coefficient, in Re=100, where boundary layer is thicker, shows bigger value near the wall, while for Re=3900, where boundary layer is thinner. Increase of Cl(rms) near the wall in thick boundary layer can be explained by increase of the lift coefficient near the wall, as a result of the perturbance of reverse pressure gradient above and below the cylinder which makes the positive fluctuations of lift coefficient bigger.

vortex shedding frequency, represented by Strouhal number, St, in thicker boundary layers (lower Reynolds numbers) increases by decreasing G/D and vice versa.

Summary and conclusions

Flow around a circular cylinder near plane has been studied in different flow regimes (Re=100, 200, 3900) with different gap ratios (G/D=∞, 1, 0.5, 0.2). Pressure distribution around the circular cylinder has been utilized to describe the variations in hydrodynamic force coefficients as well as other features of wake flow such as separation and vortex shedding phenomenon near a plane boundary. Plane wall effect on pressure distribution in different flow regimes was also assessed. it was found out that the inception of vortex shedding suppression can be deduced from pressure distribution pattern, through pressure gradient between free-stream-side and wall-side of cylinder and also the sudden decrease in maximum of positive pressure coefficient. Mean drag coefficient increases when cylinder approaches the

wall until G/D=1, but when cylinder submerges further in the plane wall's boundary layer, Cd(mean) decreases as C_{pb} decreases. Cl(rms) near the wall in thick boundary layer near the wall, increases as a result of the perturbance of reverse pressure gradient above and below the cylinder which makes the positive fluctuations of lift coefficient bigger. In a constant flow regime, upper separation point moves upward by decreasing G/D, indicates that the separation angle, θ_s decreases too. this can be described by the growing stream-wise pressure gradient induced by the gap flow.

References

[1] Zdravkovich, M. M., Flow Around Circular Cylinders, Vol 1: Fundamentals. Oxford University Press Inc, 1997.

[2] Thorn, A., "The flow past circular cylinders at low speeds". *Proceedings Royal Society,* A141, 651-69, 1933J.

[3] Homann, F., "Influence of higher viscosity on flow around cylinder" (in German). Forschung aus *dem Gebiete* des *Ingenieiuwesen,* **17,** 1-10, transl, 1952. NACA TM 1334., 1936J.

[4] Williamson, C. H. K., and Roshko, A. (1990J). Measurements of base pressure in the wake of a cylinder at low Reynolds numbers. *Zeitschriit fur Flugwissenscbeiten und Weltraumorsdwng,* 14,38-46. (Exp. 50 <*Re* < 290, *St,* FV, PS). 3, 1990J.

[5] Bearman P.W. & Zdravkovich M.M., "Flow around a circular cylinder near a plane surface", *Journal of Fluid Mechanics,* Vol. 89, pp. 33-47, 1978.

[6] Zdravkovich M.M., "Forces on a circular cylinder near a plane wall", *Applied Ocean Research.,*Vol.7, pp.197-201, 1985.

[7] Wu, M. H., Wen, C. Y., Yen, R. H., Weng, M. C., Wang, A. B., "Experimental and numerical study of the separation angle for flow around a circular cylinder at low Reynolds number", *Journal of Fluid Mechanics*, vol. 515, pp.233-260, 2004.

[8] Kirkgoz, M. S., Oner, A. A. and Akoz, M. S. , "Numerical Modeling of Interaction of a Current with a Circular Cylinder near a Rigid Bed". *Advances in Engineering Software*, 40, 1191-1199, 2009.

[9] Cao, H., Wan, D., "Application of OpenFOAM to Simulate Three-Dimensional Flows past a Single and Two Tandem Circular Cylinders" , Proceedings of the Twentieth (2010) International Offshore and Polar Engineering Conference Beijing, China, June 20-25, 2010.

[10] Williamson, C. H. K. (1991). "2-D and 3-D Aspects of the Wake of a Cylinder, and Their Relation to Wake Computations", *Lect Appl Math*, Vol 28, pp 719-751, 1991.

[11] Norberg, C., (2003), "Fluctuating lift on a circular cylinder: review and new measurements, *Journal of Fluids and Structures"* 17, 57–96, 2003.

[12] Rosetti, G. F., Vaz, G. and Fujarra, A. L. C.,(2012), "URANS Calculations For Smooth Circular Cylinder Flow In A Wide Range Of Reynolds Numbers: Solution Verification And Validation", *Journal of Fluids Engineering*, Vol. 134, 121103, 2012.

[13] Oner, A.A., Kirkgoz, M.S., Akoz, S., "Interaction of a current with a circular cylinder near a rigid bed", *Journal of Ocean Engineering*, Vol. 35, 1492-1504 , 2008.